

Extension of the strain energy updating technique
to a multilayered shell model with adaptive

Original

Extension of the strain energy updating technique
to a multilayered shell model with adaptive

displacements and fixed DOF / Icardi, Ugo. - In: JOURNAL OF AEROSPACE ENGINEERING. - ISSN 0893-1321. -
STAMPA. - 26:4(2013), pp. 842-854. [10.1061/(ASCE)AS.1943-5525.0000184]

Availability:

This version is available at: 11583/2510274 since:

Publisher:

ASCE (American Society of Civil Engineers)

Published

DOI:10.1061/(ASCE)AS.1943-5525.0000184

Terms of use:

This article is made available under terms and conditions as specified in the corresponding bibliographic description in
the repository

Publisher copyright

(Article begins on next page)

EXTENSION OF THE STRAIN ENERGY UPDATING TECHNIQUE TO A MULTILAYERED SHELL MODEL WITH “ADAPTIVE” DISPLACEMENTS AND FIXED D.O.F.

Ugo ICARDI

*Dipartimento di Ingegneria Aeronautica e Spaziale
Politecnico di Torino – Corso Duca degli Abruzzi 24, 10129 Torino, Italy
Tel : +39 (0)11 5646872; fax: +39 (0)11 5646899
E-mail addresses: ugo.icardi@polito.it*

Abstract

The strain energy updating technique (SEUPT) by the author is extended to a new zig-zag shell model with a hierarchic piecewise representation of displacements, which can adapt to the variation of solutions across the thickness. This model has the capability of being refined across the thickness without increasing the number of functional d.o.f. (the traditional mid-plane displacements and shear rotations). The purpose of SEUPT is to improve the accuracy of standard finite elements based on equivalent single-layer models with transverse shear deformations up to the level of the zig-zag model. The strain and kinetic energies and the work of external forces are updated through a post-processing iterative procedure, by starting from a local interpolation of the results of the finite element analysis. As no derivatives of in-plane stresses are involved, updating is fast. The current version of SEUPT obtains accurate predictions of interlaminar stresses from constitutive equations, so it does not require integration of local differential equilibriums, which is unwise for finite elements and can be inaccurate in certain cases. Owing to its adaptive capability, SEUPT efficiently treats thick laminated plates and shells with distinctly different properties of layers, strong anisotropy and significant transverse normal stresses and strains. Accuracy is assessed by considering the stresses under static loading and the response to blast pulse loading of undamaged and damaged sandwich shells with laminated faces. The results show that SEUPT preserves the accuracy of the zig-zag shell model and efficiently improves the accuracy of standard finite elements.

List of symbols and acronyms

Symbols	
α, β, ζ	Tri-orthogonal system of principal lines of curvature
$A^\alpha, E^\alpha, A^\beta, E^\beta, A^\zeta, E^\zeta$	Coefficients of hierarchic displacements
$C_{2\alpha}, C_{3\alpha}, C_{2\beta}, C_{3\beta}, a, b, c, d, e$	Coefficients of displacements
$u_\alpha^{(0)}(\alpha, \beta), u_\beta^{(0)}(\alpha, \beta), u_\zeta^{(0)}(\alpha, \beta),$ $\gamma_\alpha^{(0)}(\alpha, \beta), \gamma_\beta^{(0)}(\alpha, \beta)$	Functional d.o.f. (displacements and shear rotations on Ω)
$H_\alpha(\alpha, \beta, \zeta), H_\beta(\alpha, \beta, \zeta)$	Lamè coefficients
H_k	Heaviside unit step function
$\Lambda^{(k)}, \Theta^{(k)}, \Gamma^{(k)}, \Pi^{(k)}$	Stress continuity functions
$\Phi_\alpha^{(k)}, \Phi_\beta^{(k)}, \Psi_\zeta^{(k)}, \Omega_\zeta^{(k)}$	Continuity functions
$\Phi_{u1}^{(k)}, \Phi_{u9}^{(k)}, \Phi_{v1}^{(k)}, \Phi_{v9}^{(k)}, \Psi_1^{(k)}, \Psi_9^{(k)},$ $\Omega_{l1}^{(k)}, \Omega_{l8}^{(k)}$	Continuity constants
Ω	Reference middle surface
$(O\zeta^4 \dots), (O\zeta^5 \dots)$	Hierarchic contributions of displacements
$R_\alpha(\alpha, \beta), R_\beta(\alpha, \beta)$	Radii
$\sigma_{ij}, \varepsilon_{ij}$	Stress and strain components
$u_\alpha(\alpha, \beta, \zeta), u_\beta(\alpha, \beta, \zeta), u_\zeta(\alpha, \beta, \zeta)$	Displacements
Acronyms	
DLM	Discrete-layer models
ESL	Equivalent single layer models
FEM	Finite element model
FSDT	First order shear deformation theory
GL-ST	Global-local superposition technique
HM	Hierarchical models
H-ZZ1, H-ZZ2	Hierarchical zig-zag models
LWM	Layerwise models
P-C	Predictor-corrector models
PFA	Parent finite element analysis
R-ZZ	Refined zig-zag models
SEUPT	Strain energy updating technique
SB-ZZ	Sublaminar zig-zag models
SB-W-ZZ	Refined sublaminar zig-zag models
UN, DAM	Undamaged, damaged sandwiches
U6W6	Model with sixth order displacements
U6W6 UP	SEUPT with sixth order displacements
U3W4CST	Model without hierarchic contributions
ZZ	Zig-zag models

Introduction

Laminated and sandwich composites find use as primary structural components in aerospace and other branches of engineering, owing to their excellent properties and low weight. As their elastic moduli are much smaller in the thickness direction than in the in-plane direction, warping and straining deformations of the normal, transverse shear deformations and interlaminar stresses rise, which can adversely affect their failure behaviour, damage accumulation mechanisms, residual strength and service life.

In order to provide a correct representation of the cross-sectional warping and of out-of-plane stresses, the models should feature displacements that are continuous across the thickness and have appropriate discontinuous derivatives at the interfaces, since the interlaminar stresses should be continuous for keeping equilibrium. As the interlaminar shears have a significant bearing either at local or global levels, usually the piecewise variation of the in-plane displacements is accurately described. Instead, the transverse displacement is usually assumed constant, linear or parabolic, an accurate description being required just in the regions around holes, cut-outs, free edges and delamination fronts. A piecewise representation of the transverse displacement across the thickness is basic also for capturing the core crushing behaviour of sandwiches and for keeping equilibrium when temperature gradients across the thickness cause thermal stresses. Being outside the objective of this paper, no attempt is here made for reviewing the structural models that provide a correct representation of the “zig-zag” behaviour, as it is called the characteristic warping and straining deformation of the normal observed in the exact solutions (see, e.g. Pagano 1969, Ren 1987 and Wu et al. 1996). Just the displacement based models will be briefly discussed, as they are applied in the majority of studies, but also hybrid and mixed models are extensively employed (see, e.g., Wu and Liu 1995 and Soldatos and Liu 2001).

The readers are referred, among many others, to the survey papers by Savoia and Reddy 1992,1995, Reddy and Robbins 1994, Burton and Noor 1995, Altenbach 1998, Noor et al. 2000,2004 for comprehensive discussion of the models with full or partial capability of accounting for the zig-zag behaviour. Those accurately accounting for the zig-zag effects are here referred as the layerwise models (LWM). The papers by Plagianakos and Saravanos (2004), Chrysochoidis and Saravanos (2007) and Ferreira et al. (2008) are

cited as recent examples of these models. The so-called discrete-layer models (DLM), which give a separate representation in any computational layer, are the most accurate LWM to date available. As their unknowns increase with the number of computational layers, they are equally expensive as exact 3D solutions, so they could overwhelm the computational capacity if the analysis is not restricted to the local critical regions. Models that offer full 3-D modelling just in the regions where the local effects are of interest and a partial modelling capability outside are the hierarchical models (HM) (see, e.g., Barbero and Reddy 1991) and the predictor-corrector models (P-C) (see, e.g., Noor and Malik 2000, Lee and Cao 1996 and Park and Kim 2002), which assume different types of displacement fields in the same problem.

The equivalent single layer models (ESL), whose number of functional d.o.f. does not depend by the number of layers, are still extensively employed, although they violate the continuity of interlaminar stresses and do not account for the layerwise kinematics. A comprehensive review of these models is shown in the paper by Reddy and Arciniega (2004), while a comparison with LWM is shown by Matsunaga (2004).

Partial layerwise models that efficiently account for the interlaminar stresses are the so-called zig-zag models (ZZ) pioneered by Di Sciuva (1987), Di Sciuva and Icardi (1993), Xavier et al. (1993), Cho et al. (1996). These models, which have been recently retaken and extended by many researchers (see, e.g. Kapuria et al. 2003 and Oh and Cho 2004, 2007), as discussed in the recent review paper by Chakrabarti et al. (2011), are based on displacement fields similar to those of ESL, where piecewise functions enabling an *a priori* fulfilment of the stress contact conditions at the interfaces are incorporated, the so-called continuity functions. Summing up, the *a priori* fulfilment of the stress contact conditions makes ZZ more accurate than ESL, although they are based on the same functional d.o.f. and require nearly the same computational effort. The transverse displacement is usually assumed constant across the thickness, whereas the in-plane displacements are assumed to be piecewise linear or cubic. If the properties of constituent layers do not abruptly change, laminates are not extremely thick and the transverse normal stress does not have a significant bearing for keeping equilibrium, the ZZ models with a constant transverse displacement can be as accurate as DLM if the stresses are computed integrating the local differential equilibrium equations. However, as shown by Cho et al. (1996), cases exist whose stress fields computed in this way are not yet accurate enough. Furthermore, integration is unwise with finite elements, as it requires high-order shape functions. Refined

zig-zag models (R-ZZ) with a variable transverse displacement have been recently developed by Kapuria et al. (2003) and Oh and Cho (2004) for analysis of thermal stresses. Other refined zig-zag models based on a global-local superposition technique (GL-ST) have been recently developed by Li and Liu (1997) and Zhen and Wanji (2008) (17 d.o.f. plate and shell models, respectively), which accurately captures the interlaminar stresses without post-processing. Vidal and Polit (2009) recently developed a 6 d.o.f. R-ZZ beam based on GL-ST that features a parabolic variation of the transverse displacement across the thickness and a piecewise sinusoidal variation of the in-plane displacement.

Models that combine the concepts of ZZ and DLM have been developed by Averill and co-workers (see, e.g. Averill and Yip 1996), that are here referred as SB-ZZ. The analysis with these models can be carried out using a single layer, by grouping several layers, or even by subdividing a physical layer into one or more computational layers in order to capture steep stress gradients, as shown, e.g., by Mohite and Upadhyay (2007).

The author developed SB-ZZ models for analysis of local damage accumulation, of failure mechanisms and of thermoelastic problems, that are here referred as SB-W-ZZ, which fulfil also the continuity of the transverse normal stress and stress gradient at the interfaces (see Icardi 2001, 2007), as prescribed by the elasticity theory. Since the analysis of damaged sandwiches has shown that the possibility of grouping physical layers is just apparent, the author recently developed ZZ plate and shell models with the capability of being refined across the thickness without increasing the number of functional d.o.f. A hierarchical zig-zag representation of the displacements across the thickness is employed by these models, here referred as H-ZZ1 (mixed plate model) and H-ZZ2 (displacement based shell model), which does not need stacking of computational layers or post-processing for being accurate. Compared to DLM and R-ZZ models, these models have a lower memory storage occupation and a lower overall processing time, since they employ a single computational layer with few d.o.f. and the computation of hierarchic coefficients and continuity constants is fast. Their overall computational effort is also lower than with ESL and SB-ZZ models, as they do not require a long post-processing or the subdivision into a large number of computational layers required by these models.

The contribution of this paper is the extension of the strain energy updating technique (SEUPT) (see, Icardi and Ferrero 2009) to the hierarchic multilayered shell model H-ZZ2, whose functional d.o.f. are the classical mid-plane displacements and shear rotations. The purpose of SEUPT is to enable the users of standard finite elements based on shear deformation ESL models, like the First Order Shear deformation Theory (FSDT), to

improve their results up to the level of a layerwise model. Using SEUPT, accurate predictions of the bearing of the layerwise kinematics and of interlaminar strains and stresses on results are obtained starting from a FEM analysis with standard elements that disregards such effects. A spline interpolation of the FEM results is employed in a local region, which plays as an analytical solution. Basically, SEUPT consists of an iterative procedure by which the results of the finite element analysis are locally improved till they converge to the solution by the H-ZZ2 model. Since the H-ZZ2 model does not require integration of local differential equilibrium equations and has just five functional d.o.f., the updating of results by SEUPT requires a lower memory storage dimension and a lower processing time than with SB-ZZ and DLM models.

The paper is structured as follows. First, the characteristic features, the basic equations of the H-ZZ2 adaptive shell model and the modelling assumptions are discussed along with the computation of continuity functions and coefficients of hierarchic contributions, which constitute the peculiar aspects of the model. Subsequently, SEUPT is discussed and extended to the H-ZZ2 model. Then, applications to sample cases whose exact or approximate solution is available for comparisons are presented. The interlaminar stresses of simply-supported plates and shells in cylindrical bending under sinusoidal loading and their response to impulsive dynamic loading (blast pulse) are chosen as test cases, in order to assess SEUPT at global and local levels.

Structural model

Consider a multi-layered shell made of an arbitrary number of layers with different thickness and different material properties.

Preliminaries and notations

The middle surface Ω is assumed as the reference surface and the curvilinear tri-orthogonal system of the lines of principal curvature α, β and the coordinate ζ across the thickness as the reference system (see Figure 1). The elastic displacements in the α, β and ζ directions are indicated respectively as $u_\alpha, u_\beta, u_\zeta$, the strains as ε_{ij} and the stresses as σ_{ij} ($i, j = \alpha, \beta$). while the radii are indicated as $R_\alpha(\alpha, \beta), R_\beta(\alpha, \beta)$. The differentiation with respect to the spatial coordinates will be represented by the symbols $(\)_{,\alpha}, (\)_{,\beta}, (\)_{,\zeta}$. A

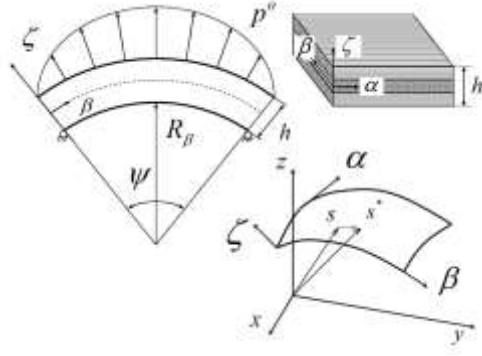


Fig. 1. Shell geometry

second-order approximation is assumed for the Lamé coefficients $H_\alpha(\alpha, \beta, \zeta)$, $H_\beta(\alpha, \beta, \zeta)$ with respect to ζ/R_α and ζ/R_β :

$$\frac{1}{H_\alpha} = \frac{1}{A_\alpha} \left(1 - \frac{\zeta}{R_\alpha} + \left(\frac{\zeta}{R_\alpha} \right)^2 \right) \quad ; \quad \frac{1}{H_\beta} = \frac{1}{A_\beta} \left(1 - \frac{\zeta}{R_\beta} + \left(\frac{\zeta}{R_\beta} \right)^2 \right) \quad (1)$$

($H_\zeta = 1$). Linear strain–displacement relations are assumed, the elastic displacements being supposed small along with their derivatives

$$\begin{aligned} \varepsilon_{\alpha\alpha} &= \frac{u_{\alpha,\alpha}}{H_\alpha} + \frac{H_{\alpha,\beta}}{H_\alpha H_\beta} u_\beta + \frac{H_{\alpha,\zeta}}{H_\alpha H_\zeta} u_\zeta \quad ; \quad \varepsilon_{\beta\beta} = \frac{u_{\beta,\beta}}{H_\beta} + \frac{H_{\beta,\alpha}}{H_\alpha H_\beta} u_\alpha + \frac{H_{\beta,\zeta}}{H_\beta H_\zeta} u_\zeta \\ \varepsilon_{\alpha\beta} &= \frac{H_\alpha}{H_\beta} \left(\frac{u_\alpha}{H_\alpha} \right)_{,\beta} + \frac{H_\beta}{H_\alpha} \left(\frac{u_\beta}{H_\beta} \right)_{,\alpha} \quad ; \quad \varepsilon_{\alpha\zeta} = \frac{H_\alpha}{H_\zeta} \left(\frac{u_\alpha}{H_\alpha} \right)_{,\zeta} + \frac{H_\zeta}{H_\alpha} \left(\frac{u_\zeta}{H_\zeta} \right)_{,\alpha} \\ \varepsilon_{\beta\zeta} &= \frac{H_\beta}{H_\zeta} \left(\frac{u_\beta}{H_\beta} \right)_{,\zeta} + \frac{H_\zeta}{H_\beta} \left(\frac{u_\zeta}{H_\zeta} \right)_{,\beta} \quad ; \quad \varepsilon_{\zeta\zeta} = \frac{1}{H_\zeta} u_{\zeta,\zeta} \end{aligned} \quad (2)$$

The quantities that belong to a generic layer k will be denoted with the suffix $^{(k)}$, the positions of the upper $^+$ and lower $^-$ surfaces of the layers will be indicated as $^{(k)}\zeta^+$ and $^{(k)}\zeta^-$.

Displacement fields (H-ZZ2 model)

The following representation of the in-plane displacements is assumed across the thickness:

$$u_\alpha(\alpha, \beta, \zeta) = \left(1 + \frac{\zeta}{R_\alpha}\right) u_\alpha^{(0)}(\alpha, \beta) - \zeta \frac{u_{\zeta, \alpha}^{(0)}(\alpha, \beta)}{A_\alpha} + \zeta \left(1 + (C_{2\alpha}(\alpha, \beta)\zeta + C_{3\alpha}(\alpha, \beta)\zeta^2)\right) \gamma_\alpha^{(0)}(\alpha, \beta) + (O \zeta^4 \dots) + \sum_{k=1}^S \Phi_\alpha^{(k)}(\alpha, \beta) (\zeta - \zeta^{(k)}) \mathbf{H}_k(\zeta - \zeta^{(k)}) \quad (3)$$

$$u_\beta(\alpha, \beta, \zeta) = \left(1 + \frac{\zeta}{R_\beta}\right) u_\beta^{(0)}(\alpha, \beta) - \zeta \frac{u_{\zeta, \beta}^{(0)}(\alpha, \beta)}{A_\beta} + \zeta \left(1 + (C_{2\beta}(\alpha, \beta)\zeta + C_{3\beta}(\alpha, \beta)\zeta^2)\right) \gamma_\beta^{(0)}(\alpha, \beta) + (O \zeta^4 \dots) + \sum_{k=1}^S \Phi_\beta^{(k)}(\alpha, \beta) (\zeta - \zeta^{(k)}) \mathbf{H}_k(\zeta - \zeta^{(k)}) \quad (4)$$

while the transverse displacement is represented as:

$$u_\zeta(\alpha, \beta, \zeta) = a(\alpha, \beta) + \zeta b(\alpha, \beta) + \zeta^2 c(\alpha, \beta) + \zeta^3 d(\alpha, \beta) + \zeta^4 e(\alpha, \beta) + (O \zeta^5 \dots) + \sum_{k=1}^{S-1} \Psi_\zeta^{(k)}(\alpha, \beta) (\zeta - \zeta^{(k)}) \mathbf{H}_k(\zeta - \zeta^{(k)}) + \sum_{k=1}^{S-1} \Omega_\zeta^{(k)}(\alpha, \beta) (\zeta - \zeta^{(k)})^2 \mathbf{H}_k(\zeta - \zeta^{(k)}) \quad (5)$$

The terms in the summations represent the zig-zag contributions which *a-priori* make continuous the transverse shear and normal stresses at the layer interfaces, as prescribed by the elasticity theory. The Heaviside unit step function \mathbf{H}_k appearing in the former equations enables the contributions of the continuity functions $\Phi_\alpha^{(k)}$, $\Phi_\beta^{(k)}$, $\Psi_\zeta^{(k)}$, $\Omega_\zeta^{(k)}$ to act from the pertinent interfaces (i.e. $\mathbf{H}_k(\zeta - \zeta^{(k)}) = 1$ for $\zeta \geq \zeta^{(k)}$ and 0 for $\zeta < \zeta^{(k)}$). The continuity functions are determined once for all for any lay-up and constituent materials by enforcing the fulfilment of the stress contact conditions at the interfaces, as outlined hereafter. The expressions of the coefficients $C_{2\alpha}, C_{3\alpha}, C_{2\beta}, C_{3\beta}$ in Eq. (3), (4) are determined by enforcing the fulfilment of the shear stress-free boundary conditions at the upper^u and lower^l free surfaces, while the coefficients b to e in Eq. (5) are determined by enforcing the boundary conditions for the transverse normal stress and stress gradient at the upper and lower bounding surfaces

$$\sigma_{\zeta\zeta} \Big|_u = p^0 \Big|_u \quad ; \quad \sigma_{\zeta\zeta} \Big|_l = p^0 \Big|_l \quad ; \quad \sigma_{\zeta\zeta, \zeta} \Big|_l = \sigma_{\zeta\zeta, \zeta} \Big|_u = 0; \quad (6)$$

p^0 being the transverse distributed loading acting at the upper and lower bounding faces, while $a \equiv u_\zeta^{(0)}(\alpha, \beta)$.

The high-order terms ($O \zeta^4 \dots$), ($O \zeta^5 \dots$) represent the hierarchic contributions that enable the displacements to adapt to the variation of solutions across the thickness, as discussed hereafter.

Characteristic features of the model

The representation of the displacements by Eqs. (3) to (5) is aimed at accurately predicting the interlaminar stresses from constitutive equations, since cases exist whose stress fields computed by integration of local equilibrium equations can be still not accurate enough, as discussed in the introductory section. To this purpose, the displacements *a priori* make continuous the interlaminar stresses at the layer interfaces with a suited choice of the continuity functions. The characteristic feature of the present model is the fulfilment also the stress contact conditions on the transverse normal stress and gradient

$$\sigma_{\zeta\zeta} |_{(+)\zeta} = \sigma_{\zeta\zeta} |_{(-)\zeta} \quad ; \quad \sigma_{\zeta\zeta,\zeta} |_{(+)\zeta} = \sigma_{\zeta\zeta,\zeta} |_{(-)\zeta} \quad (7)$$

which directly derive from the local equilibrium equations, but are usually disregarded by the models. The transverse displacement is approximated with a double zig-zag piecewise variation also with the purpose of accounting for the core crushing mechanism of sandwiches, the layerwise effects induced by temperature gradients and the role played by $\sigma_{\zeta\zeta}$ and $\varepsilon_{\zeta\zeta}$, as they can have a significant bearing on the results as discussed in the introductory section.

Although the model can be refined by choosing appropriate contributions from the higher-order terms ($O \zeta^4 \dots$), ($O \zeta^5 \dots$), as illustrated hereafter, its functional d.o.f. are just the three displacements $u_\alpha^{(0)}$, $u_\beta^{(0)}$, $u_\zeta^{(0)}$ and the two shear rotations of the normal $\gamma_\alpha^{(0)}$, $\gamma_\beta^{(0)}$ at the reference surface Ω like for classical models. The reason is that the continuity functions and the coefficients of hierarchic contributions are expressed in terms of the functional d.o.f. and of their derivatives by enforcing the stress contact conditions at the interfaces and equilibrium conditions at intermediate points across the thickness, respectively.

A shell model is chosen for generality, since laminated and sandwich plates can be particularized from it and beams can be particularized as plates in cylindrical bending.

Besides, lower order models can be obtained as particular cases. For example, the classical (CLT) and first order shear deformation (FSDT) plate models are obtained assuming a constant transverse displacement and the shear rotations as vanishing or being linear.

Continuity functions

In order to obtain the expressions of the continuity functions $\Phi_\alpha^{(k)}$, $\Phi_\beta^{(k)}$, $\Psi_\zeta^{(k)}$, $\Omega_\zeta^{(k)}$, the displacements are written in the following form:

$$u_\alpha(\alpha, \beta, \zeta) = U_\alpha(\alpha, \beta, \zeta) + \sum_{k=1}^S \Phi_\alpha^{(k)}(\alpha, \beta) (\zeta - \zeta^{(k)}) \mathbf{H}_k \quad (8)$$

$$u_\beta(\alpha, \beta, \zeta) = U_\beta(\alpha, \beta, \zeta) + \sum_{k=1}^S \Phi_\beta^{(k)}(\alpha, \beta) (\zeta - \zeta^{(k)}) \mathbf{H}_k \quad (9)$$

$$u_\zeta(\alpha, \beta, \zeta) = U_\zeta(\alpha, \beta, \zeta) + \sum_{k=1}^{S-1} \Psi_\zeta^{(k)}(\alpha, \beta) (\zeta - \zeta^{(k)}) \mathbf{H}_k + \sum_{k=1}^{S-1} \Omega_\zeta^{(k)}(\alpha, \beta) (\zeta - \zeta^{(k)})^2 \mathbf{H}_k \quad (10)$$

U_α , U_β , U_ζ being polynomials in ζ that contains the basic terms up to the third order for u_α , u_β and to the fourth order for u_ζ .

As it can be seen in a straightforward way from the interfacial stress contact conditions, the expressions of the continuity functions $\Phi_\alpha^{(k)}$, $\Phi_\beta^{(k)}$, $\Psi_\zeta^{(k)}$ involve first order

derivatives, whereas $\Omega_\zeta^{(k)}$ involve also second order derivatives. Since the stress contact conditions should be fulfilled irrespective for the displacements, their expressions should be assumed in the following form,:

$$\begin{aligned} \Phi_\alpha^{(k)} = & \Phi_{u1}^{(k)} U_{\alpha,\alpha} + \Phi_{u2}^{(k)} U_{\alpha,\beta} + \Phi_{u3}^{(k)} U_{\alpha,\zeta} + \Phi_{u4}^{(k)} U_{\beta,\alpha} + \Phi_{u5}^{(k)} U_{\beta,\beta} + \Phi_{u6}^{(k)} U_{\beta,\zeta} + \Phi_{u7}^{(k)} U_{\zeta,\alpha} + \\ & \Phi_{u8}^{(k)} U_{\zeta,\beta} + \Phi_{u9}^{(k)} U_{\zeta,\zeta} \end{aligned} \quad (11)$$

$$\begin{aligned} \Phi_\beta^{(k)} = & \Phi_{v1}^{(k)} U_{\alpha,\alpha} + \Phi_{v2}^{(k)} U_{\alpha,\beta} + \Phi_{v3}^{(k)} U_{\alpha,\zeta} + \Phi_{v4}^{(k)} U_{\beta,\alpha} + \Phi_{v5}^{(k)} U_{\beta,\beta} + \Phi_{v6}^{(k)} U_{\beta,\zeta} + \Phi_{v7}^{(k)} U_{\zeta,\alpha} + \\ & \Phi_{v8}^{(k)} U_{\zeta,\beta} + \Phi_{v9}^{(k)} U_{\zeta,\zeta} \end{aligned} \quad (12)$$

$$\begin{aligned} \Psi_\zeta^{(k)} = & \Psi_1^{(k)} U_{\alpha,\alpha} + \Psi_2^{(k)} U_{\alpha,\beta} + \Psi_3^{(k)} U_{\alpha,\zeta} + \Psi_4^{(k)} U_{\beta,\alpha} + \Psi_5^{(k)} U_{\beta,\beta} + \Psi_6^{(k)} U_{\beta,\zeta} + \\ & \Psi_7^{(k)} U_{\zeta,\alpha} + \Psi_8^{(k)} U_{\zeta,\beta} + \Psi_9^{(k)} U_{\zeta,\zeta} \end{aligned} \quad (13)$$

$$\begin{aligned}
\Omega_{\zeta}^{(k)} = & \Omega_{1}^{(k)} U_{\alpha,\alpha\alpha} + \Omega_{2}^{(k)} U_{\alpha,\alpha\beta} + \Omega_{3}^{(k)} U_{\alpha,\alpha\zeta} + \Omega_{4}^{(k)} U_{\alpha,\beta\beta} + \Omega_{5}^{(k)} U_{\alpha,\beta\zeta} + \Omega_{6}^{(k)} U_{\alpha,\zeta\zeta} + \\
& \Omega_{7}^{(k)} U_{\beta,\alpha\alpha} + \Omega_{8}^{(k)} U_{\beta,\alpha\beta} + \Omega_{9}^{(k)} U_{\beta,\alpha\zeta} + \Omega_{10}^{(k)} U_{\beta,\beta\beta} + \Omega_{11}^{(k)} U_{\beta,\beta\zeta} + \Omega_{12}^{(k)} U_{\beta,\zeta\zeta} \\
& + \Omega_{13}^{(k)} U_{\zeta,\alpha\alpha} + \Omega_{14}^{(k)} U_{\zeta,\alpha\beta} + \Omega_{15}^{(k)} U_{\zeta,\alpha\zeta} + \Omega_{16}^{(k)} U_{\zeta,\beta\beta} + \Omega_{17}^{(k)} U_{\zeta,\beta\zeta} + \Omega_{18}^{(k)} U_{\zeta,\zeta\zeta} \quad (14)
\end{aligned}$$

A system of 45 equations in the 45 unknown $\Phi_{u1}^{(k)}, \dots, \Phi_{u9}^{(k)}, \Phi_{v1}^{(k)}, \dots, \Phi_{v9}^{(k)}$,

$\Psi_1^{(k)}, \dots, \Psi_9^{(k)}, \Omega_1^{(k)}, \dots, \Omega_{18}^{(k)}$, which are the so-called continuity constants, is obtained

from Eqs. (11) to (14) by the stress contact conditions $\sigma_{j\zeta} \big|_{(+)\zeta} = \sigma_{j\zeta} \big|_{(-)\zeta}$

($j = \alpha, \beta, \zeta$), $\sigma_{\zeta\zeta,\zeta} \big|_{(+)\zeta} = \sigma_{\zeta\zeta,\zeta} \big|_{(-)\zeta}$ collecting apart the homologous displacements derivatives.

Although this system can be solved in a direct way, the second order derivatives of the displacements are initially disregarded (but few are retained, as they provide the

necessary rank) because a system of 27 equations in the 27 unknowns $\Phi_{u1}^{(k)}, \dots, \Phi_{u9}^{(k)}$,

$\Phi_{v1}^{(k)}, \dots, \Phi_{v9}^{(k)}, \Psi_1^{(k)}, \dots, \Psi_9^{(k)}$ is obtained, which makes faster the computations.

Substituting back, approximate expressions for $\Omega_1^{(k)}$ to $\Omega_{18}^{(k)}$ are determined, then the

errors are recovered by introducing new continuity functions $\Lambda^{(k)}, \Theta^{(k)}, \Gamma^{(k)}, \Pi^{(k)}$

which are determined by enforcing the continuity of stresses

$$\begin{aligned}
\sigma_{xz} &= \hat{\sigma}_{xz} + \sum_{k=1}^S \Lambda^{(k)} H^{(k)} \quad ; \quad \sigma_{yz} = \hat{\sigma}_{yz} + \sum_{k=1}^S \Theta^{(k)} H^{(k)} \\
\sigma_{zz} &= \hat{\sigma}_{zz} + \sum_{k=1}^S \Gamma^{(k)} H^{(k)} \quad ; \quad \sigma_{zz,z}^J = \hat{\sigma}_{zz,z} + \sum_{k=1}^S \Pi^{(k)} H^{(k)} \quad (15)
\end{aligned}$$

as this is numerically more efficient than the direct solution of the 45 x 45 system. In the

former equations $\hat{\sigma}_{xz}, \hat{\sigma}_{yz}, \hat{\sigma}_{zz}, \hat{\sigma}_{zz,z}$ represent the stresses computed with the approximate expressions of the continuity constants.

Of course, the expressions of the continuity functions should be computed either where the material properties of constituent layers vary, or where the representation of displacements varies.

The derivatives of displacements being unpractical by the viewpoint of finite element models, they can be converted into their primitive functions in a way that preserves their contribution to the strain energy, as shown by Icardi and Ferrero (2010, 2011).

Hierarchic terms

In order to outline the procedure for computing the coefficients of hierarchic terms, consider the following representation of displacements that focuses on the high-order contributions ($O \zeta^4 \dots$), ($O \zeta^5 \dots$):

$$u_\alpha = U_\alpha^{(3)} + A^\alpha \zeta^4 + B^\alpha \zeta^5 + C^\alpha \zeta^6 + D^\alpha \zeta^7 + E^\alpha \zeta^8 + \dots + \sum_{k=1}^S \Phi_\alpha^{(k)} \dots \quad (16)$$

$$u_\beta = U_\beta^{(3)} + A^\beta \zeta^4 + B^\beta \zeta^5 + C^\beta \zeta^6 + D^\beta \zeta^7 + E^\beta \zeta^8 + \dots + \sum_{k=1}^S \Phi_\beta^{(k)} \dots \quad (17)$$

$$u_\zeta = U_\zeta^{(4)} + A^\zeta \zeta^5 + B^\zeta \zeta^6 + C^\zeta \zeta^7 + D^\zeta \zeta^8 + E^\zeta \zeta^9 + \dots + \sum_{k=1}^S \Psi_\zeta^{(k)} \dots \quad (18)$$

In the former equations, $U_\alpha^{(3)}$, $U_\beta^{(3)}$, $U_\zeta^{(4)}$ represent the basic terms, the summations represent the zig-zag contributions and the remaining terms represent the hierarchic contributions. The unknown coefficients $A^\alpha, \dots, E^\alpha, \dots, A^\beta, \dots, E^\beta, \dots, A^\zeta, \dots, E^\zeta$ appearing in the hierarchic part of the displacements are computed as follows. The following stress derivatives are considered as examples for illustrating the procedure:

$$\sigma_{\alpha,\alpha} = [C_{11}^k U_\alpha^{(3)} + A^\alpha \zeta^4 + B^\alpha \zeta^5 + C^\alpha \zeta^6 + D^\alpha \zeta^7 + E^\alpha \zeta^8 + \dots + \sum_{k=1}^S \Phi_\alpha^{(k)} \dots]_{,\alpha} + \dots + C_{16}^k \varepsilon_{\alpha\beta,\alpha} \quad (19)$$

$$\begin{aligned} \sigma_{\alpha\beta,\beta} = & C_{16}^k \varepsilon_{\alpha\alpha,\beta} + \dots + [C_{66}^k (U_\alpha^{(3)} + A^\alpha \zeta^4 + B^\alpha \zeta^5 + C^\alpha \zeta^6 + D^\alpha \zeta^7 + \\ & E^\alpha \zeta^8 + \dots + \sum_{k=1}^S \Phi_\alpha^{(k)} \dots)_{,\beta}]_{,\beta} + [C_{66}^k (U_\beta^{(3)} + A^\beta \zeta^4 + B^\beta \zeta^5 + C^\beta \zeta^6 + \\ & D^\beta \zeta^7 + E^\beta \zeta^8 + \dots + \sum_{k=1}^S \Phi_\beta^{(k)} \dots)_{,\alpha}]_{,\beta} \end{aligned} \quad (20)$$

$$\sigma_{\alpha\zeta,\zeta} = \dots + C_{45}^k \varepsilon_{\beta\zeta,\zeta} + [C_{55}^k (U_\alpha^{(3)} + A^\alpha \zeta^4 + B^\alpha \zeta^5 + C^\alpha \zeta^6 + D^\alpha \zeta^7 + E^\alpha \zeta^8 +$$

$$\begin{aligned}
& \left(\dots + \sum_{k=1}^S \Phi_{\alpha}^{(k)} \dots \right)_{,\zeta} + C_{55}^k [U_{\zeta}^{(3)} + A^{\zeta} \zeta^4 + B^{\zeta} \zeta^5 + C^{\zeta} \zeta^6 + \\
\sigma_{\alpha\zeta,\zeta} = & \dots + C_{45}^k \varepsilon_{\beta\zeta,\zeta} + [C_{55}^k [U_{\alpha}^{(3)} + A^{\alpha} \zeta^4 + B^{\alpha} \zeta^5 + C^{\alpha} \zeta^6 + D^{\alpha} \zeta^7 + E^{\alpha} \zeta^8 + \\
& \left(\dots + \sum_{k=1}^S \Phi_{\alpha}^{(k)} \dots \right)_{,\zeta} + C_{55}^k [U_{\zeta}^{(3)} + A^{\zeta} \zeta^4 + B^{\zeta} \zeta^5 + C^{\zeta} \zeta^6 + \\
& (D^{\zeta} \zeta^7 + E^{\zeta} \zeta^8 + \dots + \sum_{k=1}^S \Psi_{\zeta}^{(k)} \dots)_{,\alpha}]_{,\zeta} \quad (21)
\end{aligned}$$

where the symbols C_{ij}^k represent the elastic coefficients. To be self-contained, just few terms have been reported in explicit form. A system of independent equations is obtained by enforcing the fulfillment of the local differential equilibrium equations at a suited number of points across the thickness, that allows to determine all the unknown coefficients of the hierarchic terms. The expressions of the coefficients A^{α} , A^{β} , A^{ζ} are determined disregarding B^{α} , B^{β} , B^{ζ} , ..., E^{ζ} , those of B^{α} , B^{β} , B^{ζ} are determined disregarding C^{α} , C^{β} , C^{ζ} , and similarly for the other coefficients, in order the higher-order models contain the lower-order ones as particular cases. The solution is obtained by an iterative process in which the starting point is represented by the solution without hierarchic terms. Once the first coefficients A^{α} , ..., E^{α} , ..., A^{β} , ..., E^{β} , ..., A^{ζ} , ..., E^{ζ} are computed, other points are chosen for computing the remaining coefficients.

In order to further refine the model, the weak form governing equations can be solved at such points, since in this way the amplitude of displacements, i.e. the solution, is recomputed across the thickness.

The overall process requires less than two seconds on a laptop computer for a 11 layer sandwich plate with simply-supported edges and sinusoidal transverse loading by starting from a linear representation of the displacements (FSDT). As a consequence, a lower computational effort than for sublaminate zig-zag models is required by the present model for achieving a comparable accuracy.

The governing equations for the present model are not reported, as they can be obtained in a straightforward way by using the standard techniques.

Strain energy updating

Suppose that a problem has been analysed by standard finite elements based on FSDT kinematics, which is here referred as the parent finite element analysis (PFA). Of course, reduced integration should be used for avoiding shear locking, or better, the inconsistent spurious constraints should be removed by the PFA finite element model. Notice that the H-ZZ2 model does not suffer from shear locking, as the true relation among bending and shear is accounted for, $u_{\zeta,\alpha}^{(0)}, u_{\zeta,\beta}^{(0)}, \gamma_{\alpha}^{(0)}, \gamma_{\beta}^{(0)}$ being kept as independent d.o.f., not like in the FSDT model where they are grouped as $\vartheta_{\alpha} = \gamma_{\alpha}^{(0)} - \zeta u_{\zeta,\alpha}^{(0)}, \vartheta_{\beta} = \gamma_{\beta}^{(0)} - \zeta u_{\zeta,\beta}^{(0)}$. The SEUPT strain energy updating procedure is a post-processing iterative procedure aimed at improving the accuracy of results of PFA up to the level of the H-ZZ2 model. As outlined hereafter, the PFA finite element solution is interpolated in the regions of interest using spline functions, then this interpolation is used to construct an updated “analytical” solution by the H-ZZ2 model. The current version of SEUPT has the following advantages.

- As just the constitutive equations are considered by the H-ZZ2 model, integration being unnecessary, no derivatives of in-plane stresses are involved, so the updating procedure is faster.
- Distinctly different properties of constituent layers, strong anisotropy, extremely thick composites, significant transverse normal stress and strain and damaged composites can be more efficiently treated by the H-ZZ2 model.
- In the current version of SEUPT, the work of the external forces is updated while computing the coefficients of the hierarchic terms, whereas this possibility was disregarded in the former version.
- Another advantage of the current version of SEUPT is the possibility of treating shells.

Implementation of SEUPT

The results at nodes or at Gauss points by PFA are used for constructing a spline interpolation of the functional d.o.f., that is here represented as

$$F(z) \cong C_0 + C_1 z^2 + C_2 z^3 + \dots \quad (z = \alpha, \beta, \zeta) \quad (22)$$

by solving $\{C\} = [V]^{-1} \{F\}$, $\{C\}$ being the vector of coefficients, $[V]$ the Vandermonde matrix and $\{F\}$ the displacements at the chosen points. The readers find all the omitted details in the standard textbooks).

Ill-conditioning is easily overcome by suitably choosing the set of interpolation points, as so many point are available in the finite element discretization as alternative choices.

Oscillations can be seen at the bounds of a sub-region if too many points are retained. In these cases, the analysis should be carried out just around the central area. As observed in the numerical applications, no oscillations and rather accurate results can be obtained using a 4x4 patch interpolation scheme around the area of interest, which results in a third-order approximation over the patches.

Differentiation $F' \cong C_1 + 2C_2z + \dots$, integration $\int F \cong \tilde{B} + C_0z + C_1/2 z^2 + \dots$ and any other operation will be carried out on the spline interpolation, so no unwise, high-order polynomials are required as finite element shape functions.

Since the updating operations are carried out only locally, they results computationally efficient as compared to other post-processing methods.

SEUPT consists of the following steps.

- i) First, the representation is rearranged for being consistent with the H-ZZZ2 model. As $\mathcal{G}_\alpha = \gamma_\alpha^{(0)} - \zeta u_{\zeta,\alpha}^{(0)}$, $\mathcal{G}_\beta = \gamma_\beta^{(0)} - \zeta u_{\zeta,\beta}^{(0)}$ are used in the FSDT elements, the shear rotations $\gamma_\alpha^{(0)}$, $\gamma_\beta^{(0)}$ that appear explicitly in the H-ZZZ2 model (along with the derivatives $u_{\zeta,\alpha}^{(0)}$, $u_{\zeta,\beta}^{(0)}$, so no shear locking rises) are recovered from the spline interpolation of \mathcal{G}_α , \mathcal{G}_β by differentiating $u_\zeta^{(0)}$.
- ii) The converted functional d.o.f. $\hat{u}_\alpha^{(0)}$, $\hat{u}_\beta^{(0)}$, $\hat{u}_\zeta^{(0)}$, $\hat{\gamma}_\alpha^{(0)}$, $\hat{\gamma}_\beta^{(0)}$ are introduced in the H-ZZZ2 model as $\hat{u}_\alpha^{(0)} + \Delta_\alpha^u$, $\hat{u}_\beta^{(0)} + \Delta_\beta^u$, $\hat{u}_\zeta^{(0)} + \Delta_\zeta^u$, $\hat{\gamma}_\alpha^{(0)} + \Delta_\alpha^\gamma$, $\hat{\gamma}_\beta^{(0)} + \Delta_\beta^\gamma$, Δ_α^u , Δ_β^u , Δ_α^γ , Δ_β^γ being the corrections that will be computed by SEUPT.
- iii) The strain energy of the FSDT model over the region of interpolation is equated that of the H-ZZZ2 model with no hierarchic terms:

$$(\mathbf{q}_i + \Delta \mathbf{q}_i)^T \mathbf{K}_{FSDT} (\mathbf{q}_i + \Delta \mathbf{q}_i) = \mathbf{q}_i^T \mathbf{K}_{HMS-ZZ} \mathbf{q}_i \quad (23)$$

In the former equation, \mathbf{q}_i represent the vector of displacements, $\mathbf{q}_i + \Delta \mathbf{q}_i$ the updated displacements and \mathbf{K} the stiffness matrix. The Penalty Function Method is used for solving. First, the continuity functions are computed, then the energy of transverse shear strains is equated. An approximate correction Δ_α^γ is obtained first by assuming all the other corrections as null. Then an approximate expression of Δ_β^γ is computed and the process is iterated till convergence. After, the remaining corrections $\Delta_\alpha^u, \Delta_\beta^u, \Delta_\zeta^u$ are computed in a similar way by considering the remaining strain energy contributions and the corrections of displacements one at a time. As FSDT disregards the strain energy due to the transverse normal stress and strain, an approximate expression of these quantities is constructed as follows.

- The interpolated transverse shear stresses by the FSDT model are derived in α, β and integrated in ζ , then an approximate expression of the transverse normal stress $\sigma_{\zeta\zeta}$ is obtained by integrating the third local differential equilibrium equation.

- After, an approximate expression of the transverse normal strain $\epsilon_{\zeta\zeta}$ is computed by the 3D stress–strain relation

$$\epsilon_{\zeta\zeta} = \sigma_{\alpha\alpha} S_{13} + \sigma_{\beta\beta} S_{23} + \sigma_{\zeta\zeta} S_{33} + \sigma_{\beta\zeta} S_{34} + \sigma_{\alpha\zeta} S_{35} + \sigma_{\alpha\beta} S_{36} \quad (24)$$

the strains being obtained deriving the interpolated displacements. In this way, improved expressions of the transverse normal strain and stress $\epsilon_{\zeta\zeta}, \sigma_{\zeta\zeta}$ are obtained from Eq. (23) using Eq. (24).

- The stresses computed at the previous iteration are interpolated by spline functions and used for the subsequent iterations.

The process is restarted from the computation of Δ_α^γ and repeated till convergence. As a measure of errors, the maximum value of the integral of any displacement divided by the area of the domain where SEUPT is carried out is used.

iv) A subdivision is chosen across the thickness for computing the hierarchic coefficients

$A^\alpha, A^\beta, A^\zeta$ by solving the local differential equilibrium equations, as discussed above.

The continuity functions are recomputed with any new hierarchic contribution. The governing equations in weak form (PLV) are solved either for refining the work of

external forces, or for the computation of the corrections Δ_λ^η . However numerical tests have shown that refinement is unnecessary for undamaged laminates and sandwiches.

The subdivisions are refined across the thickness by considering the further hierarchic contributions $B^\alpha, B^\beta, B^\zeta, \dots, E^\zeta$.

The process from iii) to iv) is continued till convergence. In this phase, the percentage of variation of the strain energy is assumed as the measure of errors.

v) The work of inertial forces is updated in a similar way for improving the dynamics of the FSDT model. The work of inertial forces, as obtained from the displacements by the finite element analysis, is interpolated by the spline functions and then equated to the one of the H-ZZ2 model in order of computing new corrections Δ_λ^η . Notice that these corrections must hold irrespective of the time evolution of the solution, which is represented as $(q_i + \Delta q_i) \mathfrak{I}(t)$. The dynamic updating of the FSDT model is obtained equating the work of inertial forces by the FSDT model to that of the H-ZZ2 model

$$(q_i + \Delta q_i)^T M_{FSDT} (q_i + \Delta q_i) = q_i^T M_{HMS-ZZ} q_i \quad (25)$$

M_{FSDT}, M_{HMS-ZZ} being the consistent mass matrices of the two models. The solution is found with an iterative process like for the strain energy.

- First the corrections $\Delta_\alpha^\gamma, \Delta_\beta^\gamma$ are computed equating the inertial work of transverse shear stresses and strains.
- Then the remaining corrections $\Delta_\alpha^u, \Delta_\beta^u, \Delta_\zeta^u$ are computed, one at a time, considering the remaining contributions to the work of inertial forces, reiterating

till convergence and still using the averaged displacements as the measure of errors, like in iii).

- The entire updating process is restarted using the last correction as the entry solution and repeated till convergence.

As shown by the numerical test, very few iterations, if not just one as occurred in most cases, are required by SEUPT for being accurate, either for the overall process i) to v), or for each sub-cycle.

Numerical applications

Accuracy and efficiency of the H-ZZZ model have been extensively assessed in the previous papers by the author. Here the capability of SEUPT of achieving comparable results without post-processing is assessed. The sample cases already considered for testing the H-ZZZ model are here presented, as for these cases the exact three-dimensional elasticity solution is available for comparisons, along with the results by various models.

Static loading is considered with the purpose of testing the accuracy of SEUPT at the local level. In this case, thick simply-supported sandwich plates and shells undergoing sinusoidal loading are considered, because stronger layerwise effects occur than for laminates. Damaged faces are also considered for having abruptly changing properties across the thickness, as owing to their intricate fields they represent a severe test. In accordance with the ply-discount theory, the damage is simulated by degrading the elastic properties. It is assumed to be spread over the entire length, although this is unrealistic. The reason is that a local distribution of the damage is difficult to treat with the closed form approaches used for comparisons. It could be noticed that, on the contrary, SEUPT can easily treat a local scale damage by the PFA finite element analysis. The overall response of SEUPT is assessed by considering panels undergoing blast pulse loading, as this loading, which can be due to an accidental cause, or explosive device, is a major hazard that can cause catastrophic failure and loss of life. Flat and doubly-curved sandwich panels are considered, since papers of theoretical, numerical or experimental nature have shown that the pressure loading hazard can be consistently reduced by using sandwich structures with honeycomb core and laminated faces. The purpose of the following numerical assessments is to test whether SEUPT, which could be successfully

employed for designing structures. It could be noticed that SEUPT is compatible with the existing finite elements packages, having compatible d.o.f., and capable of accurately predicting the overall response and the stress fields and of efficiently managing the large number of time iterations required under impulsive loading.

Analysis of static cases

First, simply-supported flat and curved sandwich panels in cylindrical bending under static sinusoidal heap loading $p^0|'' = P \sin(\pi\beta/\psi)$ are considered. For this sample cases the exact elasticity solutions by Pagano (1969) and Ren (1987) are available for comparisons in absence of damage, whereas the solution by the author (see, Icardi 2001 and Icardi and Ferrero 2011) is available for damaged cases.

The sandwich panels are treated as multilayered plates or shells made of an arbitrary number of thin layers constituting the faces and of a thick intermediate layer constituting the core, this assumption being successful in the previous studies.

Using the basic model without hierarchic terms and a constant transverse displacement, Icardi (2007) and Icardi and Ferrero (2010, 2011) have shown that the integration of local differential equilibrium equations saves the computational cost, as compared to the SB-W-ZZ model, despite it does not take a negligible fraction of processing time and memory occupation. These studies have shown that a very refined subdivision into 44 sub-layers is required by the SB-W-ZZ model, as intricate stress fields due to the distinctly different properties of core and faces occur which make apparent the advantages of sublaminate models. Owing to these effects, thick sandwich panels represent the suited test cases for assessing the accuracy of SEUPT. However, the former studies on sandwich plates have shown that the smaller effort is always required by the hierarchic model H-ZZ2 whose representation is simplified or improved as necessary. Hereafter the results predicted by SEUPT for flat and curved sandwiches are compared to those obtained in closed form by the present model.

Sandwich plate

Figure 2a shows the variation of the transverse displacement across the thickness of the undamaged sandwich plate by the exact solution and by the present model with displacements expanded up to the 6-th order (U6W6 UN). The result by the SB-W-ZZ

model (Icardi 2007) with 44 computational layers and by the present model without hierarchic contributions, i.e. with a 3-rd order expansion of the in-plane displacement and a 4-th order expansion of the transverse displacement (U4W4 CST UN) are also shown. These results are obtained in closed form within the framework of the Galertkin's method by assuming appropriate trigonometric in-plane variations for the d.o.f. Infinite radii and no variation in the direction of α are assumed in the H-ZZ2 model. Although unrealistic, a thickness ratio of 4 is considered, as it magnifies the interlaminar effects, as well as the contributions of the higher-order terms of the displacement model. The result by SEUPT is indicated as U6W6 UP UN. It corresponds to a preliminary finite element analysis (PFA) with 50 eight-node standard isoparametric plate elements in the spanwise direction and 5 elements in the width direction, whose results are updated by the present model with a 6-th order expansion of the displacements. Figure 2b presents the counterpart results when the elastic modulus E_3 of the upper face is reduced by a factor 10^{-2} (DAM), as this unrealistic test case presents intricate transverse shear stress distributions which represent a severe test for SEUPT. The transverse displacement is reported apart from a factor 10^{-5} for the undamaged case and 10^{-4} for the damaged case. Figure 2c shows the variation of the interlaminar shear stress across the thickness for the undamaged sandwich, while Figure 2d gives the same results when the upper face is damaged. Figure 2e and 2f show the variation of the transverse normal stress for undamaged and damaged sandwiches, respectively. The results are presented in the following normalized form, according to Pagano and Ren:

$$\bar{u}_\zeta(\zeta) = \frac{u_\zeta(b/2, \zeta)}{q^0 h}; \quad \bar{\sigma}_{\beta\zeta}(\zeta) = \frac{\sigma_{\beta\zeta}(0, \zeta)}{q^0 S^2 h}; \quad \bar{\sigma}_{\zeta\zeta}(\zeta) = \frac{\sigma_{\zeta\zeta}(b/2, \zeta)}{q^0} \quad (26)$$

(notice that u_ζ , $\sigma_{\zeta\zeta}$ are maximum at $\beta = b/2$, while $\sigma_{\beta\zeta}$ is maximum at $\beta = 0$). No results are presented for the in-plane displacements and stresses, as they can be easily captured also by lower order models.

The sandwich is assumed to be made with five layered face sheets made of three different materials, whose properties are:

MAT 1: $E_1=E_3=1$, $G_{13}=0.2$ (GPa), $\nu_{13}=0.25$; MAT 2: $E_1=33$, $E_3=1$, $G_{13}=8$, $\nu_{13}=0.25$; MAT 3: $E_1=25$, $E_3=1$, $G_{13}=0.5$, $\nu_{13}=0.25$. The core, which is indicated as MAT 4, has the following properties: $E_1=E_3=0.05$, $G_{13}=0.0217$, $\nu_{13}=0.15$.

The stacking sequence considered is: (MAT 1/2/3/1/3/4)_s. MAT 1 is rather weak in tension-compression and shear compared to MAT 2, whereas MAT 3 is stiff in tension-compression

but rather weak in shear. MAT 4 is very weak in tension-compression and rather weak in shear. As a consequence, strong concentrations of interlaminar stresses rise at the interfaces even in the undamaged case.

Sandwich shell

Figure 3 shows the interlaminar stress distributions for a sandwich shell in cylindrical bending. Material properties, lay-up and thickness ratio are the same as in the previous case. To enable a comparison with published results, the angle ψ is assumed equal to $\pi/3$, in such a way β traces a circumferential path of length $R_\beta\psi$ (of course, in the other direction $R_\alpha = \infty$). No results for the transverse displacement and stress are shown in this case, as they are similar to those already presented for the sandwich plate. Figure 3a gives the variation of the transverse shear stress across the thickness of a 0/90 curved panel with a radius-to-thickness ratio of 4 by the exact solution, by SEUPT (U6W6 UP), by the basic model without hierarchic contributions, as obtained by integrating the local differential equilibrium equations (U3W4 INT) and from constitutive equations (U3W4 CON). In the latter two cases, the results by the U3W4 model are obtained in closed form by the Galerkin's method, by assuming appropriate trigonometric functions for the displacements. The distribution of the transverse shear stress $\bar{\sigma}_{\beta\zeta}(\zeta)$ (SXZ) is shown in the normalized form by Eq. (26) at $\beta = 0$. Figure 3b shows the variation of this stress across the thickness of a 0/90/0 curved panel with a radius-to-thickness ratio of 4, as predicted by the above mentioned models. Figure 3c shows the variation of $\bar{\sigma}_{\beta\zeta}(\zeta)$ across the thickness of a sandwich panel with a radius-to-thickness ratio of 4, as predicted by the exact solution and by SEUPT (U6W6 UP), when the sandwich is undamaged, (DF) has a damaged upper face (E_3 reduced by a factor 10^{-2}) or (DC) the core damaged (G_{13} reduced by a factor 10^{-2}).

It can be observed from Figure 2 and 3 that SEUPT preserves the accuracy of the model used in the updating process, its results being comparable to those by the H-ZZZ2 model in closed form, while its processing time ranges from a fraction to twice the time required by the H-ZZZ2 model (the computational costs of the PFA finite element analysis have not been taken into account). As a consequence, SEUPT improves the results of a FEM analysis based on FSDT standard elements up to the accuracy level of the H-ZZZ2 model with an affordable computational effort.

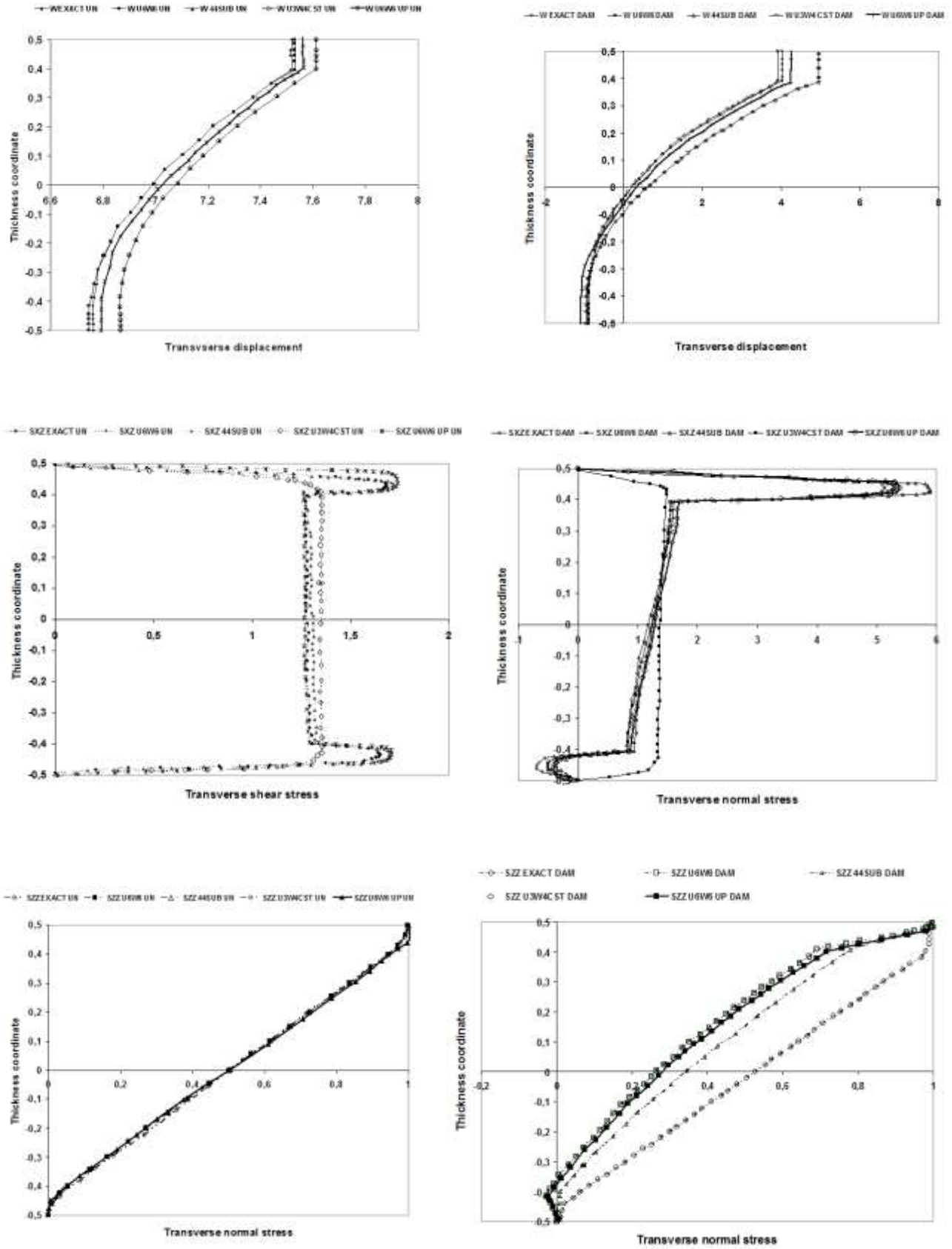


Fig. 2. Transverse displacement and interlaminar stresses of UN and DAM simply supported, flat, thick sandwich panels in cylindrical bending under sinusoidal loading

In the sample cases of Figure 3 the curved sandwich panels have been discretized in the PFA finite element analysis by 10 eight-node standard isoparametric plate elements based on FSDT and with reduced integration of the strain energy due to transverse shears in the transverse direction and 100 elements in the spanwise direction, in order to accurately represent the sinusoidal loading and the cylindrical surface of the shell. It could be noticed be that with discrete-layer models an additional fraction of time is required for matching the regions with a 3D representation with those with a partial modelling capability, while SEUPT is free from this.

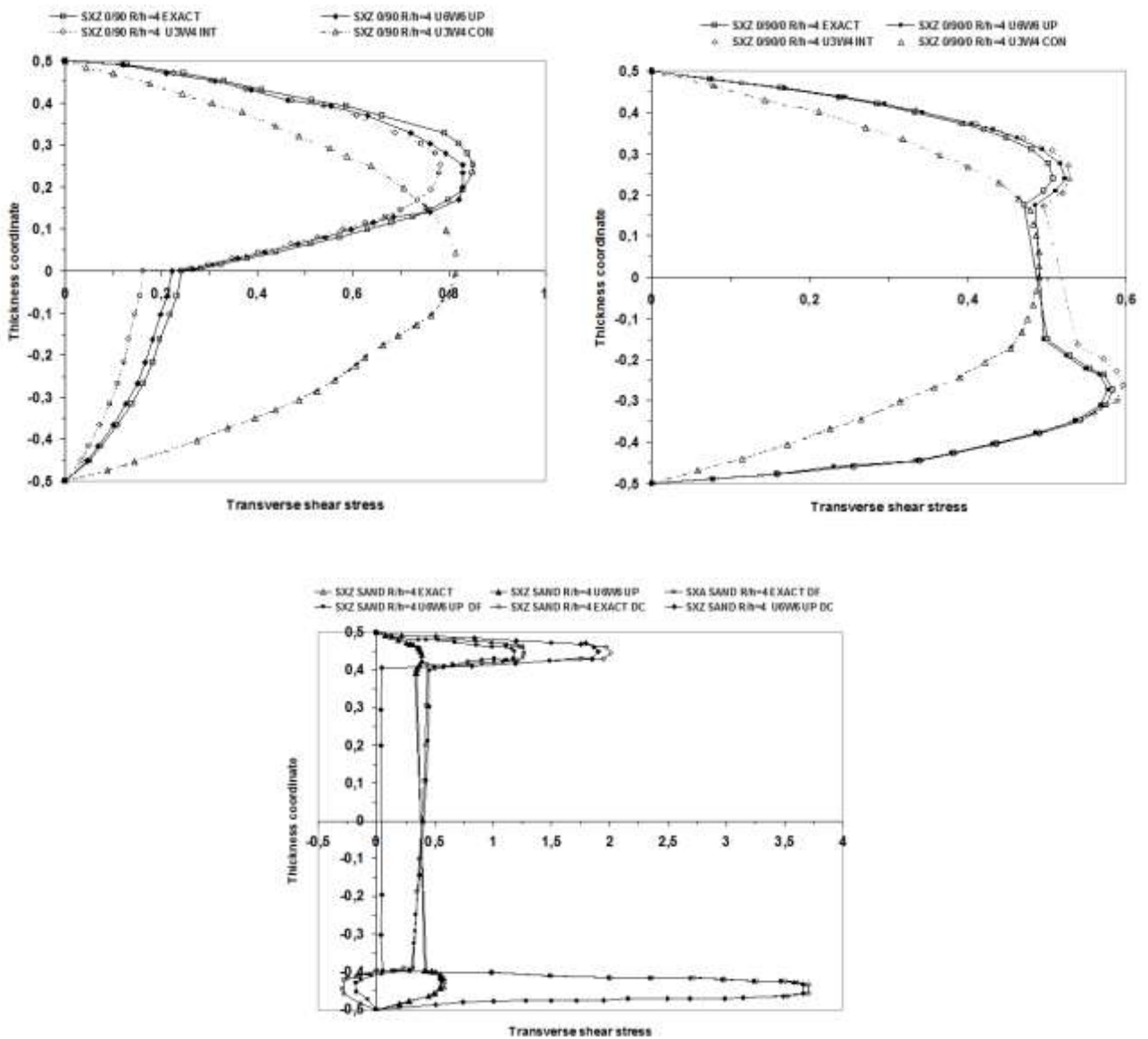


Fig. 3. Transverse shear stress distribution of cross-ply, UN, or DAM simply supported, curved sandwich panels in cylindrical bending under sinusoidal loading

Blast pulse loading

Flat and doubly-curved sandwich panels with laminated faces subject to blast loading have been investigated by Hause and Librescu (2005, 2007). In these studies, the face sheets were assimilated to equivalent anisotropic material layers free from transverse shear effects, while the core is assimilated an equivalent transversely orthotropic layer capable of carrying transverse shear stresses only. The transverse displacement was assumed uniform across the thickness, while the in-plane displacements were assumed in a form that fulfils the kinematic continuity conditions at the interfaces, but not the stress continuity conditions. The pressure loading was assumed uniform over the entire area of the panels, the front of the explosive blast pulse being supposed to be large.

The Friedländer exponential decay equation

$$P(t) = P_m \left(1 - \frac{t}{t_p}\right) e^{-a' \frac{t}{t_p}} \quad (27)$$

was used to simulate the pressure time history $P(t)$. In the former equation, P_m represents the peak pressure, a' is the decay parameter, which can be adjusted to approximate the pressure curve from blast tests, t_p is the length of the overpressure phase. Idealized cases of triangular, rectangular, sinusoidal and step pressure pulses have been considered, which can be seen as special cases of the Friedländer model.

In the present paper, square flat and doubly-curved sandwich panels with simply-supported edges, various length-to-thickness ratios subject to pulse pressure loading are considered, that correspond to cases already considered by Hause and Librescu.

A $[\mathcal{G}^\circ/\mathcal{G}^\circ/\mathcal{G}^\circ/\mathcal{G}^\circ/\mathcal{G}^\circ/\text{core}/\mathcal{G}^\circ/\mathcal{G}^\circ/\mathcal{G}^\circ/\mathcal{G}^\circ/\mathcal{G}^\circ]$ lay-up, with a specific fibre orientation \mathcal{G} defined for any application is considered. The Newmark implicit time integration scheme is used for solving the dynamic equations, because the alternative explicit time integration schemes need extremely small time steps to be stable. In all the cases presented, the effects of geometric non-linearity and damping are disregarded.

According to Hause and Librescu, the material properties of faces are chosen as:

$E_1=206.84$, $E_2=E_3=5.171$, $G_{12}=G_{13}=G_{23}=2.551$ (GPa), $\nu_{12}=\nu_{23}=0.25$, $\nu_{13}=0.22$, density 1558.35 Kg/m^3 . Those of core are: $E_1=E_2=E_3=0.138$, $G_{12}=G_{13}=0.1027$, $G_{23}=0.06205$ (GPa); ν_{ij} follows from E_{ij} and G_{ij} and the rule for transversely orthotropic media; the density is 16.3136 Kg/m^3 .

Figure 4 shows the response of a sandwich panel with a side length of 0.6096 m, a core 25.4 mm thick and each of the faces 1.905 mm thick, under a step blast pulse with an overpressure of 1.38 MPa and $\vartheta = 45^\circ$ (length-to-thickness ratio of 20.869). The central deflection as the time unfolds is reported, which is normalized to the thickness of the panel according to Hause and Librescu.

As the overall response is involved, SEUPT is carried out at selected points over the whole in-plane area of the panels. The results of a 4x4 local interpolation over a 10x100 meshing is referred as the coarse representation, that of a 8x8 scheme as the refined one. The cases indicated as Pres U6W6 UP 30° and Pres U6W6 UP 90° represent the results of SEUPT for $\vartheta = 30^\circ$, $\vartheta = 90^\circ$.

Figure 4a shows the comparison of the solution by SEUPT (coarse and refined models) to the reference solution by Hause and Librescu. In the subsequent figures, only the results by the refined model are presented. Figure 4b shows the results by SEUPT for radius-to thickness ratios of 4 and 10. Figure 4c shows the results by SEUPT

for $\vartheta = 30^\circ, 45^\circ, 90^\circ$ and a radius-to thickness ratios of 20.869. Notice that the results by SEUPT are equivalent to those by the H-ZZZ model in closed form using a 15 terms in-plane trigonometric expansion of the displacements.

The results of Figure 4 show that SEUPT predicts little less large amplitudes of the oscillation and a small delay with respect to the reference solution by Hause and Librescu. It appears by the analysis with the H-ZZZ model in closed form that a very close agreement with the reference results by Hause and Librescu is achieved if an in-plane expansion of the displacements with a single component is used and the representation across the thickness is simplified to that of FSDT. The results of Figure 4 confirm the importance of tailoring for bearing blast loads, the lowest amplitude of oscillations as the time unfolds being obtained with the orientation $\vartheta = 45^\circ$. Of course, the amplitude of deflections increases as the length-to-thickness ratio increases and the bending stiffness decreases varying ϑ . The largest amplitude is shown for $\vartheta = 90^\circ$, as to this orientation corresponds the lowest stiffness.

Figure 5 shows the response of a doubly-curved sandwich panel with radius-to-side length ratios of 0 (flat case), 0.2, 0.4, a side length of 0.420 m, a length-to-thickness ratio of 15 (T15: faces 1.5 mm thick, core 25 mm thick), under an exponential pulse profile that simulates a sonic boom ($P_m = 1.38$ Mpa, $a'/t_p = 40$, $t_p = 0.005$ s) and with $\vartheta = 45^\circ$.

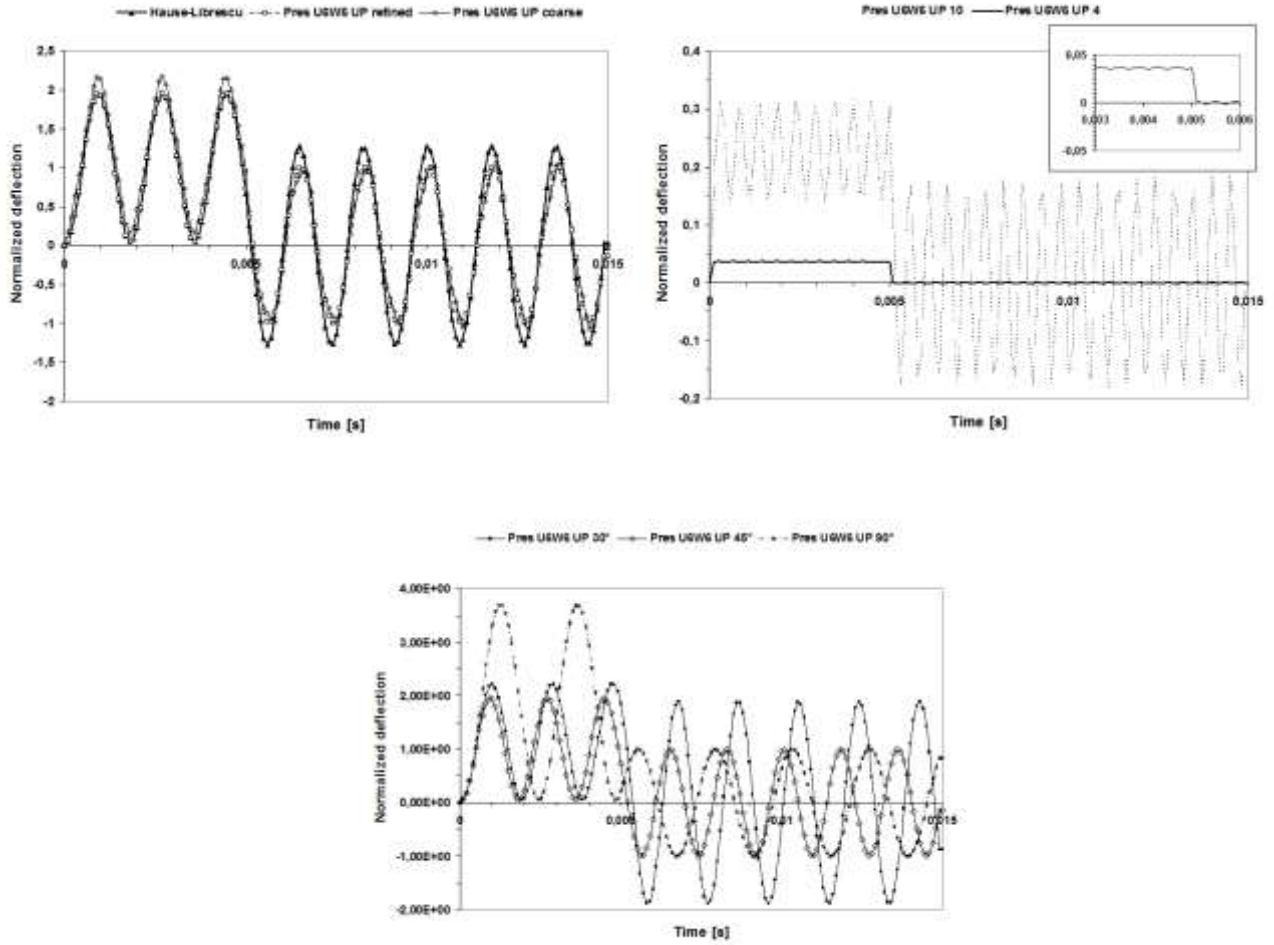


Fig. 4. Response to a pressure pulse of flat, square sandwich panels with various length-to-thickness ratios and face ply orientations

According to Hausse and Librescu, the central deflection is normalized to the static one under a uniform transverse pressure of 1.38 MPa. The same lay-up and material properties of the sample case of Figure 4 are considered. The results by SEUPT are compared to the reference results by Hausse and Librescu, for a radius-to-side length ratio (LR) of 0 (flat panel) in Figure 5a. The counterpart results for a radius-to-side length ratio of 0.2 (LR02) are given in Figure 5b, while those for 0.4 (LR04) are given in Figure 5c. The same considerations of Figure 4 still hold, about the close agreement of SEUPT with the reference results by Hausse and Librescu, though little less large amplitudes and a small delay are shown. Also in this case a better agreement with the reference solution is still shown by the analytic model U6W6 over which SEUPT is based if the transverse displacement is assumed constant across the thickness and the FSDT modelling is used across the thickness.

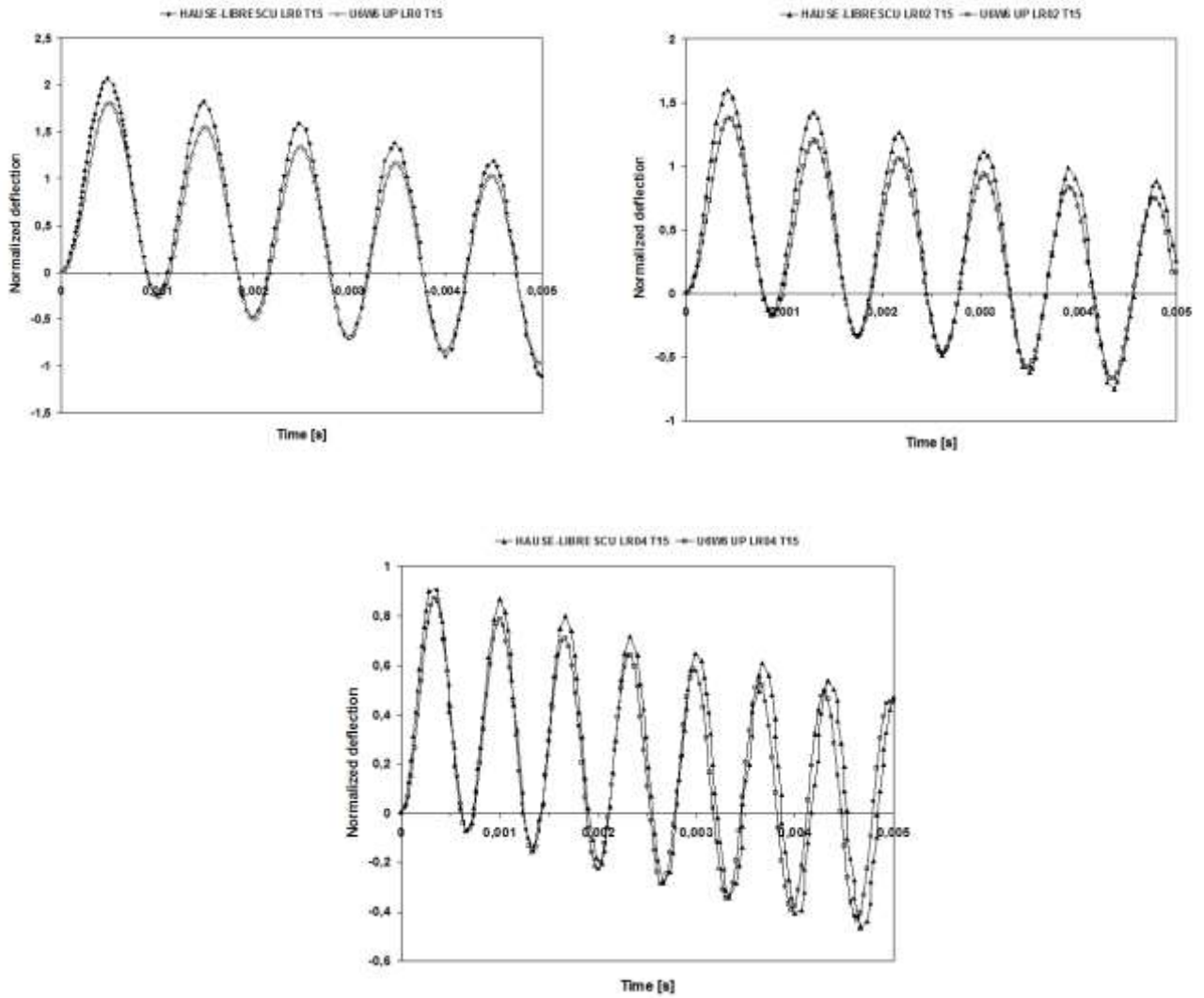


Fig. 5. Response to an axponential pressure pulse of doubly curved, square sandwich panels with various radius-to-thickness and length-to-thickness ratios

Concluding remarks

The strain energy updating technique (SEUPT), whose purpose is to improve the results of standard finite elements based on shear deformation models up to the level of a layerwise model, has been applied to a new hierarchic shell model with a piecewise zig-zag representation of the three displacements. This model accurately and efficiently predicts the interlaminar stresses without any post-processing. Due to the hierarchic representation adopted, it can be refined across the thickness without increasing the number of functional d.o.f. Compared to discrete-layer and refined zig-zag models, it requires a lower memory storage occupation and a lower overall processing time for obtaining a comparable accuracy.

SEUPT consists of an iterative procedure by which the strain energy, the work of external forces and the kinetic energy of a low order model are improved till the displacements converge to those of a high-order model with the same functional d.o.f. Results have been presented, which show the interlaminar stress distributions across the thickness of simply-supported flat and curved sandwich panels undergoing sinusoidal loading. Also dynamic results have been presented for flat and curved sandwich panels subject to pressure pulse loading.

SEUPT gives results always in a good agreement with the reference solutions and with the structural model in closed form. It effectively improves the results of standard finite elements based on simple shear deformation models up to the level of a layerwise model with an affordable computational effort. It can accurately predict either the overall response, or the stress distributions. According, SEUPT can be successfully employed for analysis of the local and global response of undamaged and damaged flat and doubly-curved sandwich panels. In particular, it can efficiently treat aircraft structures made of composite materials undergoing impulsive loadings.

References

- Altenbach H. (1998). "Theories for laminated and sandwich plates, a review." *Mech Compos Mater*; 34(3), 243–152.
- Averill R.-C., and Yip Y.-C. (1996). "An efficient thick beam theory and finite element model with zig-zag sublaminates approximations." *AIAA J* , 34, 1626-1632.
- Barbero E.-J., and Reddy J.-N. (1991). "Modeling of delamination in composite laminates using a layer-wise plate theory." *Int Jnl of Solids and Struct*, 28 (3), 373-388.
- Burton W.-S., and Noor A.-K. (1995). "Assessment of computational models for sandwich panels and shells." *Comput. Methods Appl. Mech*, 123, 125-151.
- Chakrabarti A, Chalak H.-D., Iqbal M.-A., and Sheikh A.-H. (2011) "A new FE model based on higher order zigzag theory for the analysis of laminated sandwich beam with soft core." *Composite Struct*, 93, 271–279.
- Cho M., Kim K.-O., and Kim M.-H. (1996) "Efficient higher-order shell theory for laminated composites." *Composite Struct*, 34, 197–212.
- Chrysochoidis N.-A., and Saravanos D.-A. (2007). "Generalized layerwise mechanics for the static and modal response of delaminated composite beams with active piezoelectric sensors." *Int J of Solids and Struct*, 44, 8751–8768.

- Di Sciuva M. (1987). "An improved shear deformation theory for moderately thick anisotropic shells and plates." *J Appl Mech*, 54, 589–596.
- Di Sciuva M., Icardi U. (1993). "Discrete-layer models for multilayered anisotropic shells accounting for the interlayers continuity conditions." *Meccanica* , 28, 281–291.
- Ferreira A.-J.-M., Fasshauer G.-E., Batra R.-C., and Rodrigues J.-D. (2008). "Static Deformations and Vibration Analysis of Composite and Sandwich Plates Using a Layerwise Theory and RBF-PS Discretizations with Optimal Shape Parameter." *Composite Struct*, 86, 328-343.
- Hause T, and Librescu L. (2005). "Dynamic response of anisotropic sandwich flat panels to explosive pressure pulses." *Int J Impact Eng*, 31, 607-28.
- Hause T, and Librescu L. (2007). "Dynamic response of doubly-curved anisotropic sandwich panels impacted by blast loadings." *Int J Solids Struct*, 44:6678-6700.
- Icardi U. (2001). "Higher-order zig-zag model for analysis of thick composite beams with inclusion of transverse normal stress and sublaminates approximations." *Composites: Part B Eng*, 32, 343-354.
- Icardi U. (2007). "Layerwise mixed element with sublaminates approximation and 3D zig-zag field, for analysis of local effects in laminated and sandwich composites." *Int J Num Meth Engng* , 70, 94-125.
- Icardi U., and Ferrero L. (2010). " Layerwise zig-zag model with selective refinement across the thickness." *Int Jnl Num Meth Engng*, 84, 1085-1114.
- Icardi U., and Ferrero L. (2011). " Multilayered shell model with variable representation of displacements across the thickness." *Composites Part B Eng*, 428, 18-26.
- Icardi U., and Ferrero L. (2009). "Impact analysis of sandwich composites based on a refined plate element with strain energy updating." *Composite Structures* ; 89, 35–51.
- Kapuria S., Dumir P.-C., and Ahmed A. (2003). "An efficient higher order zigzag theory for composite and sandwich beams subjected to thermal loading." *Int Jnl Solids and Struct* ,40, 6613–6631.
- Lee K.-H., and Cao L. (1996). "A predictor-corrector zig-zag model for the bending of laminated composite plates." *Int Jnl of Solids and Structs* , 33 (6), 879-897.
- Li X., and Liu D. (1997). "Generalized laminate theories based on double superposition hypothesis." *Int J Numer Meth Eng* , 40, 1197–212.
- Matsunaga H. (2004). "A comparison between 2-D single-layer and 3-D layerwise theories for computing interlaminar stresses of laminated composite and sandwich plates subjected to thermal loadings." *Composite Struct* , 64, 161–177.
- Mohite P.-M., and Upadhyay C.-S. (2007). "Region-by-region modeling of laminated composite plates." *Computers & Struct* , 85, 1808–1827.

- Noor A.-K., Burton W.-S., and Bert C.-K. (1996). "Computational models for sandwich panels and shells." *Appl Mech Rev*, 4(3), 155-99.
- Noor A.-K., and Malik M. (2000). "An assessment of modelling approaches for thermo-mechanical stress analysis of laminated composite panels." *Comput Mech*, 25, 43–58.
- Oh J., and Cho M. (2004). "A finite element based on cubic zig-zag plate theory for the prediction of thermo-electric-mechanical behaviors." *Int Jnl Solids and Struct*, 41, 1357–1375.
- Oh J, Cho M. (2007). "Higher order zig-zag theory for smart composite shells under mechanical-thermo-electric loading". *Int J Solids Struct*, 44(1), 100–127.
- Pagano N.-J. (1969). "Exact solutions for composite laminates in cylindrical bending." *J Composite Materials*, 3, 398-411.
- Park J.-W., and Kim Y.-H. (2002). "Re-analysis procedure for laminated plates using FSDT finite element method." *Comput Mech*, 29: 226–242.
- Plagianakos T.-S., and Saravanos D.-A. (2004). "High-order layerwise mechanics and finite element for the damped dynamic characteristics of sandwich composite beams." *Int J Solids and Struct*, 4, 6853–6871.
- Reddy J.-N., Robbins Jr D.-H. (1994). "Theories and computational models for composite laminates." *Appl Mech Rev*, 47, 147-169.
- Reddy J.N. (2003). "*Mechanics of laminated composite plates - Theory and analysis*." 2nd Edition, CRC Press, Boca Raton, FL, 2003.
- Reddy J.-N., and Arciniega R.-A. (2004). "Shear deformation plate and shell theories: from Stavsky to present." *Mech Adv Mater Struct*, 11, 535–82.
- Ren J.-G. (1987). "Exact solutions for laminated cylindrical shells in cylindrical bending." *Comp Sci & Tech*, 29, 169–87.
- Savoia M., and Reddy J.-N. (1992). "A variational approach to three-dimensional elasticity solutions of laminated composite plates." *J of Appl Mech*, 59, 166-175.
- Savoia M, and Reddy J.-N. (1995). "Three-dimensional thermal analysis of laminated composite plates." *Int J of Solids and Struct*, 32, 593-608.
- Soldatos K.-P., and Liu S.-L. (2001). "On the generalised plane strain deformations of thick anisotropic composite laminated plates." *Int. Jnl Solids Struct*, 38, 479–482.

Vidal P., Polit O. (2009). "A refined sine-based finite element with transverse normal deformation for the analysis of laminated beams under thermomechanical loads." *Jnl of Mech of Materials and Struct* ,4, 1127-1155.

Wu C.-P., and Liu C.-C. (1995). "Mixed finite element analysis of thick doubly curved laminated shells." *J Aerospace Eng* , 8, 43–53.

Wu C.-P., Tarn J.-Q., and Chi S.-M. (1996). "Three-dimensional analysis of doubly curved laminated shells. " *J Eng Mech* , 122(5), 391–401.

Xavier P.-B., Lee K.-H., Chew C.-H. (1993). "An improved zig-zag model for the bending of laminated composite shells. " *Compos Struct*, 26, 123–138.

Zhang Y.-X., and Yang C.-H. (2009). "Recent developments in finite element analysis for laminated composite plates." *Compos Struct* , 88, 147–157.

Zhen W., and Wanji C. (2008). "A global-local higher order theory for multilayered shells and the analysis of laminated cylindrical shell panels." *Composite Struct* , 84: 350–361.